# Monoamine oxidase-dependent endoplasmic reticulum-mitochondria dysfunction and mast cell degranulation lead to adverse cardiac remodeling in diabetes

Soni Deshwal[1], Marleen Forkink[2], Chou-Hui Hu[2], Guido Buonincontri[2], Salvatore Antonucci[1], Moises Di Sante[3], Michael P Murphy[4], Nazareno Paolocci[5,6], Daria Mochly-Rosen[7], Thomas Krieg[2], Nina Kaludercic[3]*, Fabio Di Lisa[1,3]*

[1]Department of Biomedical Sciences, University of Padova, 35131 Padova, Italy; [2]Department of Medicine, University of Cambridge, Cambridge CB2 0QQ, UK; [3]Neuroscience Institute, National Research Council of Italy (CNR), 35131 Padova, Italy; [4]Mitochondrial Biology Unit, MRC, Cambridge CB2 0XY, UK; [5]Department of Medicine, Johns Hopkins Medical Institutions, Baltimore, MD 21205, USA; [6]Department of Experimental Medicine, University of Perugia, 06123 Perugia, Italy; [7]Department of Chemical and Systems Biology, Stanford University, School of Medicine, Stanford, CA 94305-5174, USA.

*Corresponding Authors: Nina Kaludercic, PhD
Neuroscience Institute
National Research Council of Italy (CNR)
Via Ugo Bassi 58/B
35131 Padova, Italy
Tel: +39 0498271252
Fax: +39 0498276040
E-mail: nina.kaludercic@unipd.it

Fabio Di Lisa, MD
Department of Biomedical Sciences
University of Padova
Via Ugo Bassi 58/B
35131 Padova, Italy
Tel: +39 0498276132
Fax: +39 0498276040
E-mail: dilisa@bio.unipd.it

Running title: MAO, ER stress and diabetic cardiomyopathy

Word count: 3,201

Number of figures/tables: 7

**Abstract**

Monoamine oxidase (MAO) inhibitors ameliorate contractile function in diabetic animals, but the mechanisms remain unknown. Equally elusive is the interplay between the cardiomyocyte alterations induced by hyperglycemia and the accompanying inflammation. Here we show that exposure of primary cardiomyocytes to high glucose and pro-inflammatory stimuli leads to MAO-dependent increase in reactive oxygen species that causes mitochondrial dysfunction. These events occur upstream of endoplasmic reticulum (ER) stress and are abolished by the MAO inhibitor pargyline, highlighting the role of these flavoenzymes in the ER/mitochondria cross-talk. *In vivo*, streptozotocin administration to mice induced oxidative changes and ER stress in the heart, events that were abolished pargyline. Moreover, MAO inhibition prevented both mast cell degranulation and altered collagen deposition, thereby normalizing diastolic function. Taken together, these results elucidate the mechanisms underlying MAO-induced damage in diabetic cardiomyopathy and provide novel evidence for the role of MAOs in inflammation and inter-organelle communication. MAO inhibitors may be considered as a therapeutic option for diabetic complications as well as for other disorders in which mast cell degranulation is a dominant phenomenon.

**Introduction**

Cardiovascular complications account for the high morbidity and mortality in patients with type 1 and type 2 diabetes (T1D, T2D).[1] Diabetic cardiomyopathy (DCM) is a distinct myocardial disease, characterized by structural changes in the heart and diastolic/systolic dysfunction. Several factors, including reactive oxygen species (ROS) formation and mitochondrial dysfunction, contribute to hyperglycemia-induced changes and to the etiology of DCM.[2] Respiratory chain-generated superoxide[3] and $p66^{Shc}$ [4] lead to increased ROS levels characterizing mitochondria isolated from diabetic hearts or cardiomyocytes incubated with high glucose (HG).[5-7] Indeed, overexpression of ROS removing enzymes, such as MnSOD, catalase, or glutathione peroxidase decreases ROS levels and contractile abnormalities induced by diabetes.[8-11]

More recently, monoamine oxidases (MAOs) have been shown to play a major role in the oxidative stress and development of several cardiovascular pathologies, including DCM.[12-15] These flavoenzymes, localized at the outer mitochondrial membrane, exist as two isoenzymes (MAO-A and -B) and present unique features among ROS sources. The mechanism of catalysis has been elucidated and the crystal structure solved.[16, 17] During substrate degradation MAOs generate $H_2O_2$, aldehydes and ammonia,[13] thus representing a source of ROS in the heart, particularly under stress conditions. In addition, MAOs utilize specific substrates important for cardiovascular pathophysiology, such as catecholamines and serotonin. Importantly, MAOs are the only mitochondrial ROS sources for which clinically approved specific inhibitors are currently available. Nevertheless, the mechanisms of MAO-induced cardiac damage are incompletely understood, especially in the context of DCM.

Endoplasmic reticulum (ER) stress is another key determinant in cardiac physiology and pathology.[18, 19] Impairment in ER homeostasis results in ER stress, accumulation of unfolded proteins and activation of complex signaling pathways collectively termed the

unfolded protein response (UPR). If ER stress is severe or prolonged, the UPR may stimulate apoptosis, a significant feature of hypoxia, ischemia/reperfusion (I/R) injury and DCM.[18, 20] Notably, ER and mitochondria are structurally and functionally connected.[21-25] Yet, whether mitochondrial ROS formation and/or dysfunction are upstream of ER stress or vice-versa is not known.

Inflammation in the context of diabetes exacerbates cell's response to HG and is closely associated with tissue repair, scar formation and fibrosis.[26, 27] Excessive ROS formation by mitochondria and/or other sources is well-known to promote interstitial and perivascular fibrosis.[28] In addition, cardiac resident mast cell activation may contribute to fibrotic remodeling of the cardiac tissue.[29, 30] Cardiac mast cells hold secretory granules containing histamine, proteases and a variety of cytokines, growth factors, and other biologically active mediators capable of mediating tissue remodeling. Although the pathologic importance of mast cells is becoming increasingly clear, triggers leading to their activation and degranulation have not been completely elucidated.

Despite the plethora of evidence that hyperglycemia- and inflammation-induced ROS formation, mitochondrial dysfunction and ER stress contribute to the development of fibrosis and DCM,[31, 32] the precise interplay between these events remains elusive. Here, we tested the hypothesis that MAO-induced ROS formation may be the common denominator for diverse pathogenic factors contributing to changes characterizing the diabetic heart. The present study aimed to investigate whether (i) MAOs are involved in mitochondrial ROS formation and dysfunction triggered by hyperglycemia and inflammation; (ii) MAO-dependent mitochondrial derangements are upstream of ER stress occurring in the diabetic heart; (iii) MAO activity is related to cardiac fibrosis through mechanisms involving other cardiac cell types, such as mast cell degranulation.

## Results

### MAOs account for ROS formation in isolated cardiomyocytes exposed to HG and pro-inflammatory cytokine IL-1β

IL-1β, a pro-inflammatory cytokine and a regulator of the inflammatory response, is elevated in T1D and T2D.[33] Thus, to better mimic diabetic conditions *in vitro*, neonatal rat ventricular myocytes (NRVMs) were treated with HG alone or in combination with IL-1β. HG led to a significant increase in both mitochondrial (Figure 1A and B) and cytosolic $H_2O_2$ formation after 48 hours (Figure 1D and E). This rise was not due to hyperosmolarity, since identical concentrations of mannitol did not show any changes in ROS levels (Figure 1C and F, Supplementary Figure S1). Interestingly, combination of HG and IL-1β led to a further dramatic increase in $H_2O_2$ production when compared to HG or IL-1β treatment alone, indicating a synergistic effect of these stimuli in inducing ROS formation. Administration of pargyline, an inhibitor of both MAO isoforms, normalized ROS levels in these conditions (Figure 1A-F), suggesting that HG and IL-1β induce ROS formation in a MAO-dependent manner. These results were confirmed using siRNA against MAO-A, the major MAO isoform expressed in the NRVMs. After 96 hours of siRNA treatment, MAO-A protein expression was reduced by ~80% (Figure 1G and H). HG and IL-1β were unable to induce an increase in ROS formation in these siRNA-treated cells, unequivocally demonstrating the contribution of MAO to this process (Figure 1I).

To increase the translational value of the findings obtained in neonatal cells, we tested whether the same outcome holds true in adult mouse cardiomyocytes. HG showed a more prominent effect in adult cardiomyocytes, leading to a ~2-fold increase in ROS generation after only 2 hours of incubation (Figure 2A and B). Again, this effect was not due to changes in osmotic pressure (Figure 2C). However, unlike NRVMs, no further increase in oxidative stress was evident after HG/IL-1β co-treatment. Pargyline treatment reduced ROS formation

in both conditions, thus confirming that MAO plays a pivotal role in HG- and IL-1β-induced oxidative stress.

**MAO-dependent ROS generation impairs mitochondrial function in cardiomyocytes exposed to HG and IL-1β**

Next, we investigated whether increased ROS emission due to HG and IL-1β, alone or in combination, is sufficient to alter mitochondrial function in cardiomyocytes. We found that ΔΨm was markedly reduced in adult cardiomyocytes already after 5 hours of HG treatment (Figure 2D-F). This effect was further exacerbated when HG was combined with IL-1β. Since MTR accumulation in mitochondria is ΔΨm dependent, the loss of ΔΨm likely explains the absence of an additional increase in MTR signal in the adult cardiomyocytes following HG+IL1-β treatment. Unlike adult cardiomyocytes, NRVMs exposed to HG did not show any changes in ΔΨm even after 48 hours (Figure 2G). These findings prompted us to examine whether HG induces latent mitochondrial dysfunction in NRVMs. It is well established that ATP synthase can mask the loss of ΔΨm by working in a reverse mode.[34] Thus, to assess whether ATP synthase activity was compensating for the dysfunctional respiratory chain in these cells, we monitored tetramethylrhodamine methyl ester (TMRM) fluorescence intensity in the presence of the ATP synthase inhibitor oligomycin. Normal glucose (NG) or high mannitol (HM) treated cells maintained ΔΨm for up to 1 hour following oligomycin administration (Figure 2H). On the other hand, TMRM fluorescence intensity started to drop immediately in HG-treated cells upon oligomycin addition. Hence, HG induces mitochondrial dysfunction in NRVMs, but in order to maintain ΔΨm, these cells start to hydrolyze glycolytically synthesized ATP by reversing the activity of the ATP synthase. Pre-treatment with pargyline maintained ΔΨm in both neonatal and adult cardiomyocytes, indicating that MAO-generated ROS trigger mitochondrial dysfunction in cardiomyocytes treated with HG and IL-1β.

**MAO inhibition prevents the activation of UPR in cardiomyocytes treated with HG and IL-1β**

Besides oxidative stress and inflammation, ER stress is another key contributor to DCM development.[20] ER stress may be mediated by increased oxidative stress and vice-versa.[21, 35, 36] Here we sought to determine whether HG and IL-1β perturb ER function in a MAO-dependent manner. Expression levels of GRP78/BiP, an ER chaperone and a central regulator of UPR, were ~3 fold upregulated in the presence of HG and HG-IL1β (Figure 3A and B). Furthermore, the expression of growth arrest- and DNA damage-inducible protein GADD34 (Figure 3C) and transcription factor ATF4 (Figure 3D), two proteins downstream of GRP78, was also significantly upregulated. Accordingly, phosphorylation levels of IRE1α, an ER transmembrane kinase, were increased as well in these cells, further confirming the activation of the UPR (Figure 3E). Importantly, MAO inhibition prevented the UPR activation induced by HG and IL-1β in adult cardiomyocytes (Figure 3A-E). Thus, the effects produced by MAO-dependent ROS formation go well beyond mitochondria, affecting also ER homeostasis to activate the UPR. Furthermore, excessive mitochondrial ROS formation and dysfunction are upstream of ER stress, at least under present experimental conditions. Next, we tested whether MAO takes part in the cell damage triggered by well-known ER stressors, such as tunicamycin and thapsigargin. The latter compounds led to severe ER stress that MAO inhibition was not able to abolish (Figure 3F, Supplementary Figure S2A). Pargyline treatment partially reduced tunicamycin-induced ROS formation (Supplementary Figure S2B); however, it did not prevent cell death caused by either compound (Supplementary Figure S2C). These results show that MAO is central to ROS-induced ER stress/UPR activation. Accordingly, MAO inhibition effectively prevents ER stress when UPR is activated by oxidative stress, but not when ER stress is triggered by other redox-

independent mechanisms, such as inhibition of N-linked glycosylation or depletion of ER $Ca^{2+}$ stores.

**MAO inhibition prevents diastolic dysfunction in streptozotocin-treated mice**

To investigate whether MAO contributes to the cardiac dysfunction associated with diabetes, MAO inhibitor pargyline was administered to streptozotocin (STZ) treated mice. Pressure-volume (PV) relationships revealed that STZ-mice have smaller hearts with a significant reduction in left ventricle (LV) chamber volumes (Figure 4A and Table 1). STZ-mice treated with pargyline showed an improvement in cardiac morphology, although the differences were not statistically significant between the two groups. Heart rate and cardiac output were similar between groups (Table 1). We found that, although ejection fraction (an index of systolic function) was also unaffected in STZ-mice (Figure 4B), $dP/dt_{max}$ and $dP/dt_{min}$ (load-dependent indices of contractility and relaxation) showed a trend to a decrease in STZ-treated mice (Table 1). These data suggest that, whereas systolic function is unaffected after 12 weeks from diabetes induction, STZ mice can still develop overt systolic impairment with time. At the same time, there was an increase in diastolic stiffness, an index of diastolic dysfunction, which was 4.6-fold higher in the diabetic mice (Figure 4C). Hence, our findings are congruent with several clinical reports showing that diastolic dysfunction is an early event in diabetic cardiomyopathy in which systolic impairment will eventually occur at later stages.[31] Importantly, pargyline administration prevented diastolic stiffening in STZ-mice, suggesting that MAO contributes to diastolic dysfunction in T1D.

**Oxidative stress and ER stress are reduced in STZ hearts upon pargyline treatment**

We next examined whether MAO contributes to oxidative and ER stress in T1D *in vivo*. Formation of 4-hydroxynonenal (4-HNE), an aldehyde product of lipid peroxidation, was measured as an index of oxidative stress. In line with our *in vitro* data, we found increased levels of 4-HNE in STZ hearts (Figure 4D and E). This was accompanied by

impaired ER homeostasis as demonstrated by the induction of UPR associated proteins ATF4 (Figure 4F and G) and GADD34 (Figure 4F and H). Pargyline administration to diabetic mice completely prevented these alterations, suggesting that hyperglycemia-induced changes in diabetic hearts lead to enhanced MAO-mediated ROS generation, eventually prompting cardiac redox imbalance and activation of the UPR.

**MAO activity triggers cardiac fibrosis and mast cell degranulation in STZ hearts**

Cardiac fibrosis is one of the underlying causes of diastolic dysfunction and a major feature of DCM.[2, 37] We observed that STZ-treated hearts displayed 4-fold increase in collagen deposition as compared to normal hearts (Figure 5A and B). Interestingly, pargyline treatment abrogated this change, demonstrating MAO inhibitors' ability to prevent fibrosis progression in T1D animals. Since mast cell degranulation is involved in fibrosis development and known to play a key role in the inflammatory process by releasing a number of pro-inflammatory and pro-fibrotic factors,[30, 38] we next assessed cardiac mast cell density and level of degranulation in STZ vs control mice (Figure 5C). Although mast cell density was similar between the groups (Figure 5D), the extent of degranulation was markedly higher in STZ mice (Figure 5E). Pargyline treatment prevented this event in T1D mice. Thus, MAO-induced ROS production can trigger cardiac mast cell activation and degranulation. This phenomenon, in turn, contributes to the remodeling of the extracellular matrix, ultimately resulting in LV fibrosis and dysfunction.

**Discussion**

The present results demonstrate that MAO-induced ROS formation causes mitochondrial dysfunction, ER stress and fibrosis, factors that ultimately promote DCM development (Figure 6). Mitochondrial and cytosolic ROS formation that ensues upon cardiomyocyte incubation with HG and pro-inflammatory cytokine IL-1β is MAO-dependent and occurs upstream of mitochondrial dysfunction and ER stress. Importantly, the improvement in diastolic stiffness elicited by MAO inhibition *in vivo* is accompanied by a reduction in interstitial fibrosis, establishing a previously unappreciated mechanistic link between cardiac fibrosis and mast cell degranulation that is MAO-dependent.

Many alterations in cellular and mitochondrial metabolism observed during the development of DCM are associated with increased ROS levels. In this setting, cardiac impairment is not caused by hyperglycemia *per se*; rather, oxidative stress and inflammation lead to cardiovascular complications. Mitochondrial ROS formation and dysfunction lead to the production of IL-1β via the inflammasome pathway.[39] Yet, whether and how IL-1β can induce mitochondrial ROS formation has not been reported. Here we show that IL-1β, in combination with HG, induces mitochondrial ROS formation and dysfunction in a MAO-dependent manner. Other studies have shown that diabetes-induced mitochondrial dysfunction and ROS formation occur through calpain[40] and O-linked β-N-acetylglucosamine glycosylation.[41] Our results strongly support the central role of mitochondrial ROS formation and dysfunction in DCM, indicating MAO activity as an upstream event or part of an amplification pathway exacerbating mitochondrial dysfunction.

Hyperglycemia and inflammation induce ER stress and consequently trigger the UPR.[32, 42] Severe and/or prolonged ER stress plays a predominant role in the pathogenesis of multiple cardiovascular diseases.[18] There is an association between oxidative and ER stress, but whether mitochondrial ROS formation is upstream of ER stress or vice-versa was not

clear. Activation of the UPR under stress conditions leads to impaired $Ca^{2+}$ and redox homeostasis.[21, 36] Hence, oxidative stress is increased leading to impaired mitochondrial function. However, the opposite also holds true. In fact, aberrant ROS formation and alterations in mitochondrial structure and function may affect ER homeostasis.[35] Here we show that MAO activity primarily accounts for impaired ER homeostasis and activation of the UPR. HG- and inflammation-induced ROS formation and mitochondrial dysfunction in cardiomyocytes are upstream of ER stress, given that abrogation of MAO-dependent ROS formation was sufficient to abolish the UPR in those conditions. These findings highlight a novel role for these flavoenzymes as a key linchpin between excessive ROS formation and ER stress. Moreover, our present data show that MAO inhibition was not sufficient to protect cells from damage when ER stress was induced directly and occurred upstream of mitochondrial ROS formation. This outcome is likely due to the fact that both tunicamycin and thapsigargin lead to a more severe ER stress in comparison to our *in vitro* diabetic model. On the other hand, it is plausible that tunicamycin- and thapsigargin-induced ER stress causes mitochondrial dysfunction, oxidative stress and cell death in a MAO-independent manner. Indeed, ER stress can induce cell death as a consequence of SR $Ca^{2+}$ release and PTP opening.[43]

Many studies have suggested that oxidative stress plays a critical role in the development of DCM.[2] Our data indicate that MAOs are responsible for the oxidative stress, ER stress and fibrosis underlying cardiac dysfunction in T1D. Another study identified MAO-A as an important source of ROS in STZ-treated rats, suggesting that its inhibition may improve cardiac contractility.[15] These Authors focused on the later stages of DCM, characterized by reduced heart rate and contractility, and likely associated with reduced ejection fraction and dilation. However, most recent clinical reports on DCM describe a phenotype that differs from dilated cardiomyopathy.[44] The typical diabetic patient suffering

from DCM falls into the category of heart failure with preserved ejection fraction (HFpEF), presenting a small LV cavity, normal systolic LV ejection fraction, thick LV walls, elevated LV filling pressures and diastolic dysfunction.[44] Therefore, it's important to assess whether MAOs contribute to the early impairment in diabetic hearts, represented by diastolic dysfunction. Here we provide unprecedented evidence that diastolic stiffness observed in STZ mice is prevented by MAO inhibition. These findings are of major clinical relevance because several heart failure drugs showed positive outcomes in heart failure patients with reduced ejection fraction, but the outcome was neutral in HFpEF.[44] Currently, treatment of DCM with HFpEF phenotype is limited to diuretics and lifestyle modification. Therefore, our results highlight the therapeutic potential of MAO inhibitors in the latter cohort of diabetic/HFpEF patients, while providing key mechanistic advancement concerning the mechanisms underlying MAO-induced changes in the diabetic heart. Future studies must be designed *ad hoc* to test whether MAO inhibition affords benefits even when instituted after the onset of diastolic dysfunction, i.e., at later stages of DCM.

Collagen deposition and extracellular matrix remodeling result in the stiffening of the cardiac tissue and diastolic dysfunction. Mast cells contain pro-inflammatory, hypertrophic and pro-fibrogenic factors and their degranulation is a key-contributing factor in heart failure pathogenesis, irrespective of the etiology.[30] However, the exact mechanisms leading to mast cell degranulation are unclear, partly owing to the multiplicity of environmental stressors they are sensitive to. Oxidative stress is a trigger for mast cell activation,[45] but until now no study has identified specific ROS source liable for mast cell degranulation in DCM. Here we report that MAO activity triggers mast cell degranulation in STZ-mice, thus providing a mechanistic link between these mitochondrial flavoenzymes, inflammation and fibrosis in DCM. Cardiac mast cells are also important for myofilament $Ca^{2+}$ sensitivity following myocardial infarction,[46] raising the question whether mast cells can directly regulate

cardiomyocte contractile machinery in DCM. Interestingly, mast cell stabilizer nedocromil has been shown to only partially prevent structural and functional changes in the diabetic heart.[38] It is therefore tempting to hypothesize that the stronger protection observed in our study is due to the synergistic effects of MAO inhibition on cardiomyocytes and mast cells. Further studies are necessary to elucidate the exact mechanisms linking MAO activation and mast cell degranulation.

Besides $H_2O_2$ formation, MAOs are also a source of reactive aldehydes and ammonia.[13] Stimulation of mitochondrial ALDH2 activity, the enzyme responsible for aldehyde conversion into the corresponding carboxylic acids, improves mitochondrial function and reduces cardiac damage in several models of cardiac injury, including T1D.[47] It is plausible that MAO inhibition in diabetes abolishes the detrimental effects of these reactive aldehydes as well. Another aspect of our study that warrants further, in-depth investigation is the exact mechanism leading to the upregulation of MAO activity in diabetes. Although we did not observe changes in MAO protein expression (Supplementary Figures S3 and S4), increased substrate availability and/or post-translational modifications might account for enhanced MAO activity. Augmented MAO-dependent norepinephrine and dopamine degradation contributes to heart failure in pressure-overloaded mice.[12, 14] In addition, histamine has been shown to trigger MAO-dependent impairment in vasorelaxation,[48] although the signaling pathway linking histamine receptors and/or metabolism with MAO activity was not elucidated. Considering that histamine, dopamine and serotonin are all contained in mast cell granules, it is possible that these substrates are responsible for MAO activation, at least in this cell type.

In conclusion, the present findings identify MAOs as major vehicles of damage during the hyperglycemic and pro-inflammatory states characterizing DCM. By extension, MAO inhibitors that are currently used in the clinic for treating depression or Parkinson's disease

should be considered as a therapeutic option for diabetes and its complications as well as for other disorders in which mast cell degranulation is a dominant phenomenon.

## Materials and Methods

### Animals

All animal studies were performed using male C57BL6/J mice (6-7 weeks of age; Charles River Laboratories, UK). T1D was induced with STZ intraperitoneally for five consecutive days (50 mg/kg/day in citrate buffer pH 4.5). Animals were then randomized and treated either with vehicle or MAO inhibitor pargyline (50 mg/kg/day). Blood glucose levels were measured twice a month using glucose meter (OneTouch Ultra 2) and mice with blood glucose levels ≥17 mM were considered diabetic. Animal studies were performed in accordance with relevant guidelines and regulations and were approved by the Italian Ministry of Health and the University of Cambridge.

### *In vivo* cardiac function

*In vivo* cardiac function was assessed using MRI-calibrated PV loops. First, a MRI scan was performed as previously described to assess systolic function.[49, 50] Mice were quickly anaesthetized with isoflurane followed by a 70 mg/kg intraperitoneal injection of pentobarbital. After endotracheal intubation for mechanical ventilation (Harvard apparatus, Holliston, MA), mice underwent closed-chest catheterization of the left ventricle via the carotid artery. PV data was acquired using a Transonic ADV 500 system (iWorx 125 Systems Inc., NH). Before PV loop analysis, volumes were smoothed (smoothing kernel of 4 ms), and calibrated using the MRI data. The maximum and minimum volumes obtained with the catheter were matched to the MRI-derived LV volumes. Summary pressure and diastolic stiffness values were derived using Labscribe 2 (iWorx 125 Systems Inc., NH).

### Primary myocytes studies

NRVMs were isolated from 1-3 days old rats as previously described[14] and plated at the density of 100,000 cells/ml in minimum essential media (MEM) supplemented with FBS 10%, antibiotics and non-essential amino acids. Cells were maintained at 37°C, 5% $CO_2$. The

medium was changed to MEM supplemented with 1% FBS after 24 hours. Adult mouse ventricular myocytes were isolated from the hearts of 12 weeks old C57Bl6/J mice as previously described.[51] Collagenase-digested isolated myocytes were incubated in buffer with increasing concentrations of $Ca^{2+}$, achieving a final concentration of 1.2 mM $Ca^{2+}$ as in MEM culture media (Life Technologies). Cells were seeded at 25,000 rod-shaped myocytes/ml on coverslips coated with laminin. After 1 hour incubation at 37°C, 2% $CO_2$, culture media was replaced to remove unattached cells.

ROS formation in NRVMs was measured using the genetically encoded $H_2O_2$ sensitive mito-HyPer or cyto-HyPer plasmids (Evrogen) or 25 nM Mitotracker Red (MTR, CM-$H_2$XRos, Life Technologies). Cells were transfected with the calcium phosphate method and treated for 48 hours in following conditions: NG 5 mM, HG 25 mM or HM 25 mM in presence or absence of 25 ng/ml rat IL-1β (Sigma). To inhibit MAO activity cells were either pre-treated with 100 μM pargyline (Sigma) or transfected with scramble or MAO-A siRNA (Ambion). Adult cardiomyocytes were loaded with 250 nM MTR, washed and treated as above for 2 hours. Images were captured using fluorescence microscope (Leica). Analysis and fluorescence intensities were determined using computer-assisted image analysis systems (ImageJ, NIH).

To measure mitochondrial membrane potential (ΔΨm) cardiomyocytes were incubated with NG, HG and IL-1β as above for 5 hours and then loaded with 25 nM TMRM, a cell-permeant dye sequestered by active mitochondria, in presence of 1.6 μM cyclosporin H. Images were collected using a fluorescence microscope (Leica) before and after the addition of 6 μM oligomycin and 2.5 μM FCCP. Images were analyzed and fluorescence intensities determined using computer-assisted image analysis systems (ImageJ, NIH). Results are expressed as ΔF ($F_0/F_{FCCP}$).

**Histology**

Hearts were fixed in 10% formalin overnight, embedded in paraffin and sectioned at 5 μm thickness. To detect collagen deposition, sections were stained with Masson's Trichrome (Bio-Optica, Milan, Italy). Photomicrographs of the sections were evaluated for interstitial collagen fractions using computer-assisted image analysis systems (Adobe Photoshop).

Metachromatic staining with toluidine blue (0.1%, pH 2.3, for 3 minutes) was employed to detect mast cell density and degranulation.[30] Mast cell density was determined counting the total number of mast cells per field. Mast cell degranulation was expressed as the number of degranulating mast cells normalized to total number of mast cells.

**Real time-PCR**

Total RNA was extracted from NRVMs using Trizol reagent (Invitrogen). Isolated RNA was reverse transcribed to cDNA using random hexamers, dNTPs and SuperScript III reverse transcriptase (Invitrogen), following manufacturer's protocol and amplified by PCR.

**Western blot**

Cardiomyocytes or heart tissue were homogenized in lysis buffer containing protease and phosphatase inhibitors. Protein concentration was determined using BCA protein assay (Pierce). Proteins were separated using SDS-PAGE (Invitrogen) and transferred to nitrocellulose membrane (Bio-Rad). Following incubation with primary and secondary HRP-conjugated antibody (Bio-Rad), bands were detected using KODAK Image station 4000 MM PRO and analyzed using Gel-Pro software.

**Statistical analysis**

All values are expressed as mean ± SEM. Comparison between groups was performed by one-way or two-way ANOVA, followed by Tukey's *post hoc* multiple comparison for normally distributed data and non-parametric Dunn's test for not normally distributed data.

Comparisons between two groups were performed using non-paired two-tailed Student's t-test. A value of $p<0.05$ was considered significant.

**Acknowledgements**

We thank Dr. Suresh Palaniyandi for helpful discussion and advice. This work was supported by the EFSD/Sanofi research grant (NK), Leducq Transatlantic Network of Excellence, MIUR and University of Padova Strategico grant (FDL), CNR (NK and FDL), Medical Research Council UK (MC_U105663142) and Wellcome Trust Investigator award (110159/Z/15/Z to MPM). DMR was supported by NIH (HL52141). NK and MDS are Fellows of the Leducq Transatlantic Networks of Excellence. SD and MF were supported by the Marie Sklodowska Curie fellowship through the RADOX ITN network.

## Conflict of Interests

The authors declare no conflicts of interests.

**References**


1. Grundy SM, Benjamin IJ, Burke GL, Chait A, Eckel RH, Howard BV*, et al.* Diabetes and cardiovascular disease: a statement for healthcare professionals from the American Heart Association. *Circulation* 1999, **100**(10)**:** 1134-1146.

2. Bugger H, Abel ED. Molecular mechanisms of diabetic cardiomyopathy. *Diabetologia* 2014, **57**(4)**:** 660-671.

3. Nishikawa T, Edelstein D, Du XL, Yamagishi S, Matsumura T, Kaneda Y*, et al.* Normalizing mitochondrial superoxide production blocks three pathways of hyperglycaemic damage. *Nature* 2000, **404**(6779)**:** 787-790.

4. Di Lisa F, Giorgio M, Ferdinandy P, Schulz R. New aspects of p66Shc in ischaemia reperfusion injury and other cardiovascular diseases. *Br J Pharmacol* 2017, **174**(12)**:** 1690-1703.

5. Shen E, Li Y, Li Y, Shan L, Zhu H, Feng Q*, et al.* Rac1 is required for cardiomyocyte apoptosis during hyperglycemia. *Diabetes* 2009, **58**(10)**:** 2386-2395.

6. Dabkowski ER, Williamson CL, Bukowski VC, Chapman RS, Leonard SS, Peer CJ*, et al.* Diabetic cardiomyopathy-associated dysfunction in spatially distinct mitochondrial subpopulations. *Am J Physiol Heart Circ Physiol* 2009, **296**(2)**:** H359-369.

7. Boudina S, Sena S, Theobald H, Sheng X, Wright JJ, Hu XX*, et al.* Mitochondrial energetics in the heart in obesity-related diabetes: direct evidence for increased uncoupled respiration and activation of uncoupling proteins. *Diabetes* 2007, **56**(10)**:** 2457-2466.

8. Baseler WA, Dabkowski ER, Jagannathan R, Thapa D, Nichols CE, Shepherd DL*, et al.* Reversal of mitochondrial proteomic loss in Type 1 diabetic heart with overexpression of phospholipid hydroperoxide glutathione peroxidase. *Am J Physiol Regul Integr Comp Physiol* 2013, **304**(7)**:** R553-565.

9. Matsushima S, Kinugawa S, Ide T, Matsusaka H, Inoue N, Ohta Y*, et al.* Overexpression of glutathione peroxidase attenuates myocardial remodeling and preserves diastolic function in diabetic heart. *Am J Physiol Heart Circ Physiol* 2006, **291**(5)**:** H2237-2245.

10. Ye G, Metreveli NS, Donthi RV, Xia S, Xu M, Carlson EC*, et al.* Catalase protects cardiomyocyte function in models of type 1 and type 2 diabetes. *Diabetes* 2004, **53**(5)**:** 1336-1343.

11. Shen X, Zheng S, Metreveli NS, Epstein PN. Protection of cardiac mitochondria by overexpression of MnSOD reduces diabetic cardiomyopathy. *Diabetes* 2006, **55**(3)**:** 798-805.

12. Kaludercic N, Carpi A, Nagayama T, Sivakumaran V, Zhu G, Lai EW*, et al.* Monoamine oxidase B prompts mitochondrial and cardiac dysfunction in pressure overloaded hearts. *Antioxid Redox Signal* 2014, **20**(2)**:** 267-280.

13. Kaludercic N, Mialet-Perez J, Paolocci N, Parini A, Di Lisa F. Monoamine oxidases as sources of oxidants in the heart. *J Mol Cell Cardiol* 2014, **73:** 34-42.

14. Kaludercic N, Takimoto E, Nagayama T, Feng N, Lai EW, Bedja D*, et al.* Monoamine oxidase A-mediated enhanced catabolism of norepinephrine contributes to adverse remodeling and pump failure in hearts with pressure overload. *Circ Res* 2010, **106**(1)**:** 193-202.

15. Umbarkar P, Singh S, Arkat S, Bodhankar SL, Lohidasan S, Sitasawad SL. Monoamine oxidase-A is an important source of oxidative stress and promotes cardiac dysfunction, apoptosis, and fibrosis in diabetic cardiomyopathy. *Free Radic Biol Med* 2015, **87:** 263-273.

16. Binda C, Newton-Vinson P, Hubalek F, Edmondson DE, Mattevi A. Structure of human monoamine oxidase B, a drug target for the treatment of neurological disorders. *Nat Struct Biol* 2002, **9**(1)**:** 22-26.

17. Son SY, Ma J, Kondou Y, Yoshimura M, Yamashita E, Tsukihara T. Structure of human monoamine oxidase A at 2.2-A resolution: the control of opening the entry for substrates/inhibitors. *Proc Natl Acad Sci U S A* 2008, **105**(15)**:** 5739-5744.

18. Groenendyk J, Sreenivasaiah PK, Kim DH, Agellon LB, Michalak M. Biology of endoplasmic reticulum stress in the heart. *Circ Res* 2010, **107**(10)**:** 1185-1197.

19. Miki T, Miura T, Hotta H, Tanno M, Yano T, Sato T*, et al.* Endoplasmic reticulum stress in diabetic hearts abolishes erythropoietin-induced myocardial protection by impairment of phospho-glycogen synthase kinase-3beta-mediated suppression of mitochondrial permeability transition. *Diabetes* 2009, **58**(12)**:** 2863-2872.

20. Yang L, Zhao D, Ren J, Yang J. Endoplasmic reticulum stress and protein quality control in diabetic cardiomyopathy. *Biochim Biophys Acta* 2015, **1852**(2)**:** 209-218.

21. Arruda AP, Pers BM, Parlakgul G, Guney E, Inouye K, Hotamisligil GS. Chronic enrichment of hepatic endoplasmic reticulum-mitochondria contact leads to mitochondrial dysfunction in obesity. *Nat Med* 2014, **20**(12)**:** 1427-1435.

22. Dorn GW, 2nd, Song M, Walsh K. Functional implications of mitofusin 2-mediated mitochondrial-SR tethering. *J Mol Cell Cardiol* 2015, **78:** 123-128.

23. de Brito OM, Scorrano L. Mitofusin 2 tethers endoplasmic reticulum to mitochondria. *Nature* 2008, **456**(7222)**:** 605-610.

24. Lewis SC, Uchiyama LF, Nunnari J. ER-mitochondria contacts couple mtDNA synthesis with mitochondrial division in human cells. *Science* 2016, **353**(6296)**:** aaf5549.

25. Sebastian D, Hernandez-Alvarez MI, Segales J, Sorianello E, Munoz JP, Sala D*, et al.* Mitofusin 2 (Mfn2) links mitochondrial and endoplasmic reticulum function with insulin signaling and is essential for normal glucose homeostasis. *Proc Natl Acad Sci U S A* 2012, **109**(14)**:** 5523-5528.

26. Lafuente N, Matesanz N, Azcutia V, Romacho T, Nevado J, Rodriguez-Manas L*, et al.* The deleterious effect of high concentrations of D-glucose requires pro-inflammatory preconditioning. *J Hypertens* 2008, **26**(3)**:** 478-485.

27. Kanasaki K, Taduri G, Koya D. Diabetic nephropathy: the role of inflammation in fibroblast activation and kidney fibrosis. *Front Endocrinol (Lausanne)* 2013, **4:** 7.

28. Richter K, Kietzmann T. Reactive oxygen species and fibrosis: further evidence of a significant liaison. *Cell Tissue Res* 2016, **365**(3)**:** 591-605.

29. Levick SP, Melendez GC, Plante E, McLarty JL, Brower GL, Janicki JS. Cardiac mast cells: the centrepiece in adverse myocardial remodelling. *Cardiovasc Res* 2011, **89**(1)**:** 12-19.

30. Palaniyandi SS, Inagaki K, Mochly-Rosen D. Mast cells and epsilonPKC: a role in cardiac remodeling in hypertension-induced heart failure. *J Mol Cell Cardiol* 2008, **45**(6)**:** 779-786.

31. Boudina S, Abel ED. Diabetic cardiomyopathy, causes and effects. *Rev Endocr Metab Disord* 2010, **11**(1)**:** 31-39.

32. Hotamisligil GS. Endoplasmic reticulum stress and the inflammatory basis of metabolic disease. *Cell* 2010, **140**(6)**:** 900-917.

33. Larsen CM, Faulenbach M, Vaag A, Volund A, Ehses JA, Seifert B*, et al.* Interleukin-1-receptor antagonist in type 2 diabetes mellitus. *N Engl J Med* 2007, **356**(15)**:** 1517-1526.

34. Irwin WA, Bergamin N, Sabatelli P, Reggiani C, Megighian A, Merlini L*, et al.* Mitochondrial dysfunction and apoptosis in myopathic mice with collagen VI deficiency. *Nat Genet* 2003, **35**(4)**:** 367-371.

35. Malhotra JD, Miao H, Zhang K, Wolfson A, Pennathur S, Pipe SW*, et al.* Antioxidants reduce endoplasmic reticulum stress and improve protein secretion. *Proc Natl Acad Sci U S A* 2008, **105**(47)**:** 18525-18530.

36. Safiedeen Z, Rodriguez-Gomez I, Vergori L, Soleti R, Vaithilingam D, Douma I*, et al.* Temporal Cross Talk Between Endoplasmic Reticulum and Mitochondria Regulates Oxidative Stress and Mediates Microparticle-Induced Endothelial Dysfunction. *Antioxid Redox Signal* 2017, **26**(1)**:** 15-27.

37. Miki T, Yuda S, Kouzu H, Miura T. Diabetic cardiomyopathy: pathophysiology and clinical features. *Heart Fail Rev* 2013, **18**(2)**:** 149-166.

38. Huang ZG, Jin Q, Fan M, Cong XL, Han SF, Gao H*, et al.* Myocardial remodeling in diabetic cardiomyopathy associated with cardiac mast cell activation. *PLoS One* 2013, **8**(3)**:** e60827.

39. Zhou R, Yazdi AS, Menu P, Tschopp J. A role for mitochondria in NLRP3 inflammasome activation. *Nature* 2011, **469**(7329)**:** 221-225.

40. Ni R, Zheng D, Xiong S, Hill DJ, Sun T, Gardiner RB*, et al.* Mitochondrial Calpain-1 Disrupts ATP Synthase and Induces Superoxide Generation in Type 1 Diabetic Hearts: A Novel Mechanism Contributing to Diabetic Cardiomyopathy. *Diabetes* 2016, **65**(1)**:** 255-268.

41. Hu Y, Suarez J, Fricovsky E, Wang H, Scott BT, Trauger SA*, et al.* Increased enzymatic O-GlcNAcylation of mitochondrial proteins impairs mitochondrial function in cardiac myocytes exposed to high glucose. *J Biol Chem* 2009, **284**(1)**:** 547-555.

42. Liu Z, Zhao N, Zhu H, Zhu S, Pan S, Xu J*, et al.* Circulating interleukin-1beta promotes endoplasmic reticulum stress-induced myocytes apoptosis in diabetic cardiomyopathy via interleukin-1 receptor-associated kinase-2. *Cardiovasc Diabetol* 2015, **14:** 125.

43. Lee GH, Lee HY, Li B, Kim HR, Chae HJ. Bax inhibitor-1-mediated inhibition of mitochondrial Ca2+ intake regulates mitochondrial permeability transition pore opening and cell death. *Sci Rep* 2014, **4:** 5194.

44. Seferovic PM, Paulus WJ. Clinical diabetic cardiomyopathy: a two-faced disease with restrictive and dilated phenotypes. *Eur Heart J* 2015, **36**(27)**:** 1718-1727, 1727a-1727c.

45. Koda K, Salazar-Rodriguez M, Corti F, Chan NY, Estephan R, Silver RB*, et al.* Aldehyde dehydrogenase activation prevents reperfusion arrhythmias by inhibiting local renin release from cardiac mast cells. *Circulation* 2010, **122**(8)**:** 771-781.

46. Ngkelo A, Richart A, Kirk JA, Bonnin P, Vilar J, Lemitre M*, et al.* Mast cells regulate myofilament calcium sensitization and heart function after myocardial infarction. *J Exp Med* 2016, **213**(7)**:** 1353-1374.

47. Zhang Y, Babcock SA, Hu N, Maris JR, Wang H, Ren J. Mitochondrial aldehyde dehydrogenase (ALDH2) protects against streptozotocin-induced diabetic cardiomyopathy: role of GSK3beta and mitochondrial function. *BMC Med* 2012, **10:** 40.

48. Sturza A, Leisegang MS, Babelova A, Schroder K, Benkhoff S, Loot AE*, et al.* Monoamine oxidases are mediators of endothelial dysfunction in the mouse aorta. *Hypertension* 2013, **62**(1)**:** 140-146.

49. Buonincontri G, Methner C, Carpenter TA, Hawkes RC, Sawiak SJ, Krieg T. MRI and PET in mouse models of myocardial infarction. *J Vis Exp* 2013(82)**:** e50806.

50. Buonincontri G, Methner C, Krieg T, Carpenter TA, Sawiak SJ. Functional assessment of the mouse heart by MRI with a 1-min acquisition. *NMR Biomed* 2014, **27**(6)**:** 733-737.

51. O'Connell TD, Rodrigo MC, Simpson PC. Isolation and culture of adult mouse cardiac myocytes. *Methods Mol Biol* 2007, **357:** 271-296.

**Figure legends**

**Figure 1. Effects of MAO inhibition on HG and pro-inflammatory cytokine IL-1β induced ROS formation in NRVMs.** ROS formation was measured with genetically encoded $H_2O_2$ sensitive probe HyPer targeted either to mitochondria (A, B) or to the cytosol (D, E) upon NRVMs treatment with NG or HG in the absence or presence of IL-1β, and with or without pargyline (n=4 per each group). Effects of HM, as osmotic control, were assessed on mitochondrial (C) and cytosolic (F) $H_2O_2$ formation (n=3 per each group). Effects of MAO-A knockdown were assessed on MAO-A protein expression (G and H) and ROS formation upon treatment with NG or HG in the absence or presence of IL-1β (I, n=3 per each group). Approximately 100 cells were analyzed per condition in each experiment and all the experiments were performed in triplicates. Data are expressed as mean ± SEM. Two-way ANOVA test followed by post hoc Tukey's test (*$p<0.05$ vs NG vehicle, #$p<0.05$ vs HG vehicle and §$p<0.05$ vs HG-IL1β).

**Figure 2. Effects of MAO inhibition on ROS formation and mitochondrial membrane potential in cardiac myocytes exposed to HG and/or IL-1β.** ROS formation was assessed with the fluorescent dye MTR in adult cardiomyocytes treated with NG or HG in the absence or presence of IL-1β, and with or without pargyline (A and B, n=3 per each group). Effects of the osmotic control HM on ROS formation (C). Mitochondrial membrane potential was measured in adult cardiomyocytes with the fluorescent dye TMRM in the same conditions as above (D-F, n=3 per each group). Mitochondrial membrane potential in neonatal cardiomyocytes was measured following 48 hour treatment with NG or HG in the absence or presence of IL-1β (G, n=3 per each group). Kinetic measurements were performed to follow TMRM fluorescence intensity following additions of oligomycin and FCCP, indicated by arrows (H). Approximately 100 cells were analyzed per condition in each experiment and all the experiments were performed in triplicates. Data are expressed as mean ± SEM. Two-way

ANOVA test followed by post hoc Tukey's test (*p<0.05 vs NG vehicle, #p<0.05 vs HG and §p<0.05 vs HG+IL-1β vehicle).

**Figure 3. Effects of MAO inhibition on ER stress in adult cardiomyocytes exposed to HG and/or IL-1β.** Representative western blots (A) and quantification of the protein expression of ER stress markers GRP78 (B), GADD34 (C), ATF4 (D) and phosphorylation levels of IRE1α (E) were assessed in adult cardiomyocytes treated with HG and IL-1β with (white) or without (black) pargyline. Protein expression was normalized to total protein determined by Red Ponceau staining (n=5 per each group). Effects of the MAO inhibitor pargyline and the chemical chaperone TUDCA on tunicamycin-induced upregulation of ER stress markers (F, n=3 per each group). All the experiments were performed in triplicates. Data are expressed as mean ± SEM. Two-way ANOVA test followed by post hoc Tukey's test (*p<0.05 vs NG vehicle, #p<0.05 vs HG and §p<0.05 vs HG+IL-1β vehicle).

**Figure 4. Characterization of LV function, oxidative and ER stress in vehicle- and pargyline-treated STZ-mice.** Representative pressure-volume loops from control (blue, n=6), STZ (black, n=8), control+pargyline (green, n=4) and STZ+pargyline (red, n=10) treated mice (A). Ejection fraction (B) and diastolic stiffness (C) were determined in vehicle (black bars) or pargyline (white bars) treated control and STZ mice. Control n=6, STZ n=8, control+pargyline n=4 and STZ+pargyline n=10. Levels of 4-HNE (D, E) were assessed in heart tissue lysates from control, STZ and STZ+pargyline treated mice. Protein levels were normalized to total protein content determined by Red Ponceau (n=5 per each group). Representative Western blot for ER stress markers performed in heart tissue lysates from control, STZ and STZ+pargyline treated mice (F). ATF4 (G) and GADD34 (H) band intensities were quantified and normalized to total protein content determined by Red Ponceau (n=5 per each group). PV loop analysis was carried out by an observer blinded to the

experimental conditions. Data are expressed as mean ± SEM. Two-way ANOVA test followed by post hoc Tukey's test (*p<0.05 vs CT vehicle, #p<0.05 vs STZ vehicle).

**Figure 5. Effects of MAO inhibition on cardiac fibrosis and mast cell degranulation in STZ-mice.** Representative images of Masson's trichrome staining from control and STZ mice, showing collagen deposition in blue (A). The quantification data are expressed as percentage of fibrotic vs total cardiac tissue (B). Black and white bars represent vehicle and pargyline treated mice, respectively (Control n=10, control+pargyline n=5, STZ n=12, STZ+pargyline n=15). Representative images of toluidine blue staining of cardiac tissue from indicated experimental groups (C). Red arrows indicate intact mast cells, and black arrows indicate actively degranulating mast cells. Quantification of mast cell density (D) and mast cell degranulation (E). Results are expressed as number of mast cells per field and percentage of degranulating mast cells vs total number of mast cells, respectively. (Control n=10, control+pargyline n=5, STZ n=12, STZ+pargyline n=15). Analysis was carried out by an observer blinded to the experimental conditions. Data are expressed as mean ± SEM. Two-way ANOVA test followed by *post hoc* Tukey's test (*p<0.05 vs control vehicle, #p<0.05 vs STZ vehicle).

**Figure 6. Schematic representation of the effects elicited by MAO-dependent oxidative stress in diabetic cardiomyopathy.** Hyperglycemia and pro-inflammatory stimuli result in enhanced mitochondrial MAO-dependent $H_2O_2$ formation that, in turn, targets mitochondria to induce mitochondrial dysfunction. These events occur upstream of the impairment in ER homeostasis and accumulation of unfolded proteins in the ER lumen. The consequent activation of the UPR through three ER stress branches, namely IRE1α, PERK and ATF6, leads to protein translation attenuation, upregulation of chaperones and activation of ERAD machinery. Moreover, MAO-dependent oxidative stress *in vivo* contributes to mast cell degranulation and cardiac fibrosis, ultimately resulting in diastolic dysfunction in type 1

diabetes. Administration of the MAO inhibitor pargyline prevents exacerbated ROS formation and restores mitochondrial and ER homeostasis. In addition, MAO inhibition abolishes mast cell degranulation and fibrosis, thus improving LV diastolic function. *ATF4: activation transcription factor 4, ATF6: activation transcription factor 6, BiP: binding immunoglobulin protein, ER: endoplasmic reticulum, ERAD: ER associated degradation, eIF2α: eukaryotic initiation factor 2α, IRE1α: inositol-requiring enzyme 1α, IL-1β: interleukin 1β, MAO: monoamine oxidase, PERK: protein kinase R-like endoplasmic reticulum kinase, ROS: reactive oxygen species, UPR: unfolded protein response.*

**Table 1. Glycemic and hemodynamic parameters measured in STZ-mice.**

EDV: end-diastolic volume, ESV: end-systolic volume, SV: stoke volume, EF: ejection fraction, CO: cardiac output, ESP: end-systolic pressure, EDP: end diastolic pressure. Data are expressed as mean ± SEM. Two-way ANOVA test followed by *post hoc* Tukey's test (*p<0.005 vs Control, †p<0.005 vs STZ).

| | **Control (n=6)** | **Control+Parg (n=4)** | **STZ (n=8)** | **STZ+Parg (n=10)** |
|---|---|---|---|---|
| **Glucose (mmol/l)** | 10.20±1.40 | 8.60±0.40 | 32.20±30* | 32.10±3.10* |
| **Body weight (g)** | 33.10±2.70 | 32.40±2.00 | 25.50±4.30 | 24.20±5.30 |
| **Heart rate (bpm)** | 380.56±20.42 | 446.59±21.90 | 350.57±16.58 | 343.83±1.94 |
| **EDV (µl)** | 65.66±9.43 | 70.50±2.60 | 47.62±3.52* | 50.70±2.87* |
| **ESV (µl)** | 21.50±4.28 | 27.00±1.41 | 14.87±1.74 | 15.30±1.49 |
| **SV (µl)** | 44.16±5.31 | 43.50±2.38 | 32.87±2.12* | 35.20±2.11* |
| **EF (%)** | 68.01±2.06 | 61.75±2.07 | 69.34±1.76 | 69.82±1.88 |
| **Diastolic stiffness (1/µl)** | 0.0158±0.005 | 0.010±0.004 | 0.069±0.009* | 0.0331±0.007† |
| **ESP (mmHg)** | 82.66±2.39 | 91.63±5.72 | 67.47±5.67 | 76.20±1.94 |
| **EDP (mmHg)** | 8.58±1.53 | 5.98±1.79 | 9.21±2.20 | 10.32±1.75 |
| **$dP/dt_{max}$ (mmHg/s)** | 5487.40±430.94 | 7120.29±522.16 | 4101.85±645.78 | 4713.28±316.7 |
| **$dP/dt_{min}$ (mmHg/s)** | -5930.80±389.2 | -7161.70±804.36 | -4001.30±886.90 | -4500.29±885.7 |
| **Efficiency (%)** | 73.35±4.15 | 70.37±17.02 | 76.22±6.62 | 74.06±5.36 |

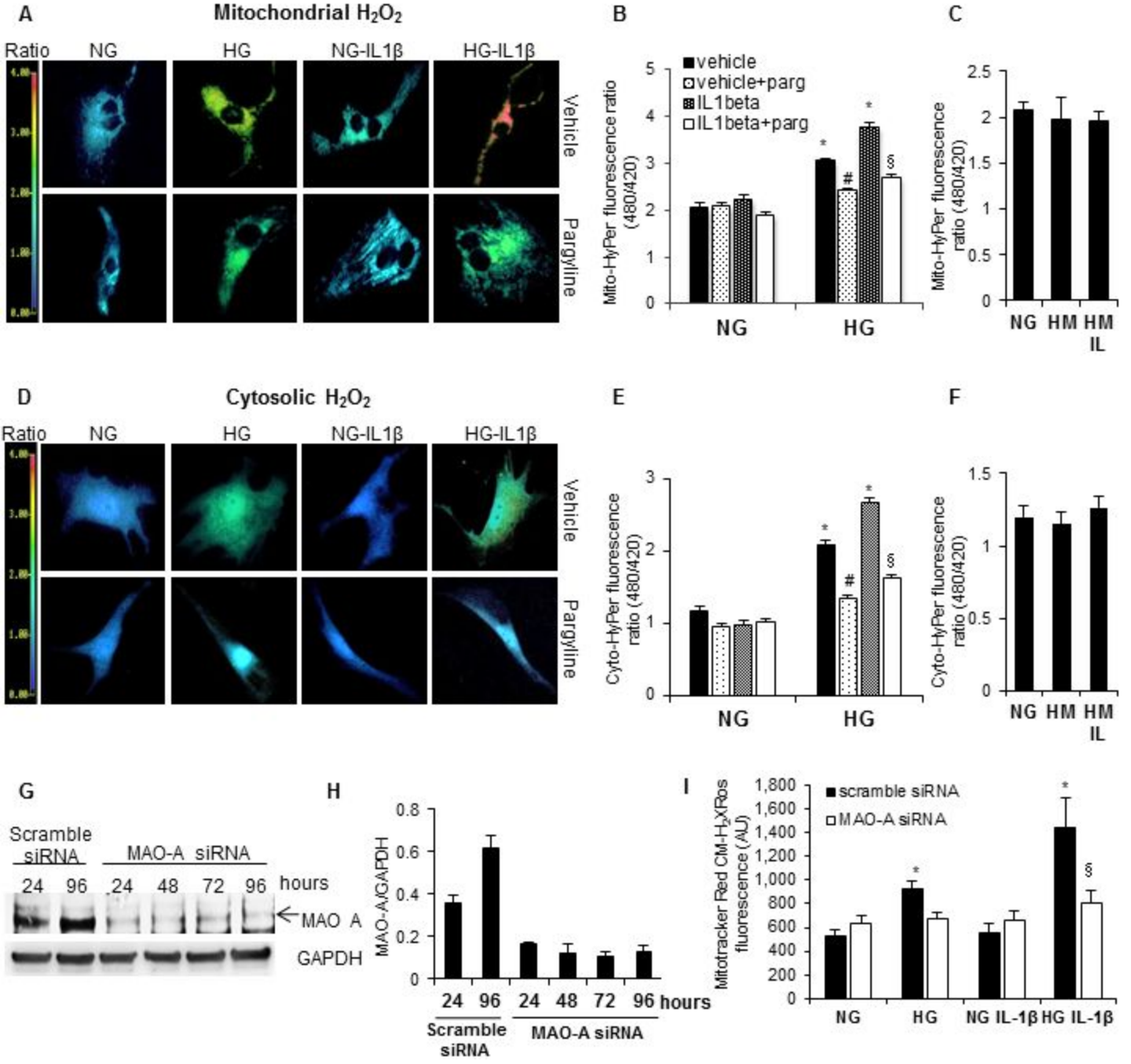
A
Mitochondrial $H_2O_2$
Ratio
NG
HG
NG-IL1β
HG-IL1β
Vehicle
Pargyline
B
vehicle
vehicle+parg
IL1beta
IL1beta+parg
Mito-HyPer fluorescence ratio (480/420)
NG
HG
C
Mito-HyPer fluorescence ratio (480/420)
NG
HM
HM IL
D
Cytosolic $H_2O_2$
Ratio
NG
HG
NG-IL1β
HG-IL1β
Vehicle
Pargyline
E
Cyto-HyPer fluorescence ratio (480/420)
NG
HG
F
Cyto-HyPer fluorescence ratio (480/420)
NG
HM
HM IL
G
Scramble siRNA
MAO-A siRNA
24
96
24
48
72
96
hours
MAO A
GAPDH
H
MAO-A/GAPDH
24
96
24
48
72
96
hours
Scramble siRNA
MAO-A siRNA
I
scramble siRNA
MAO-A siRNA
Mitotracker Red CM-$H_2$XRos fluorescence (AU)
NG
HG
NG IL-1β
HG IL-1β

**FIGURE 1**

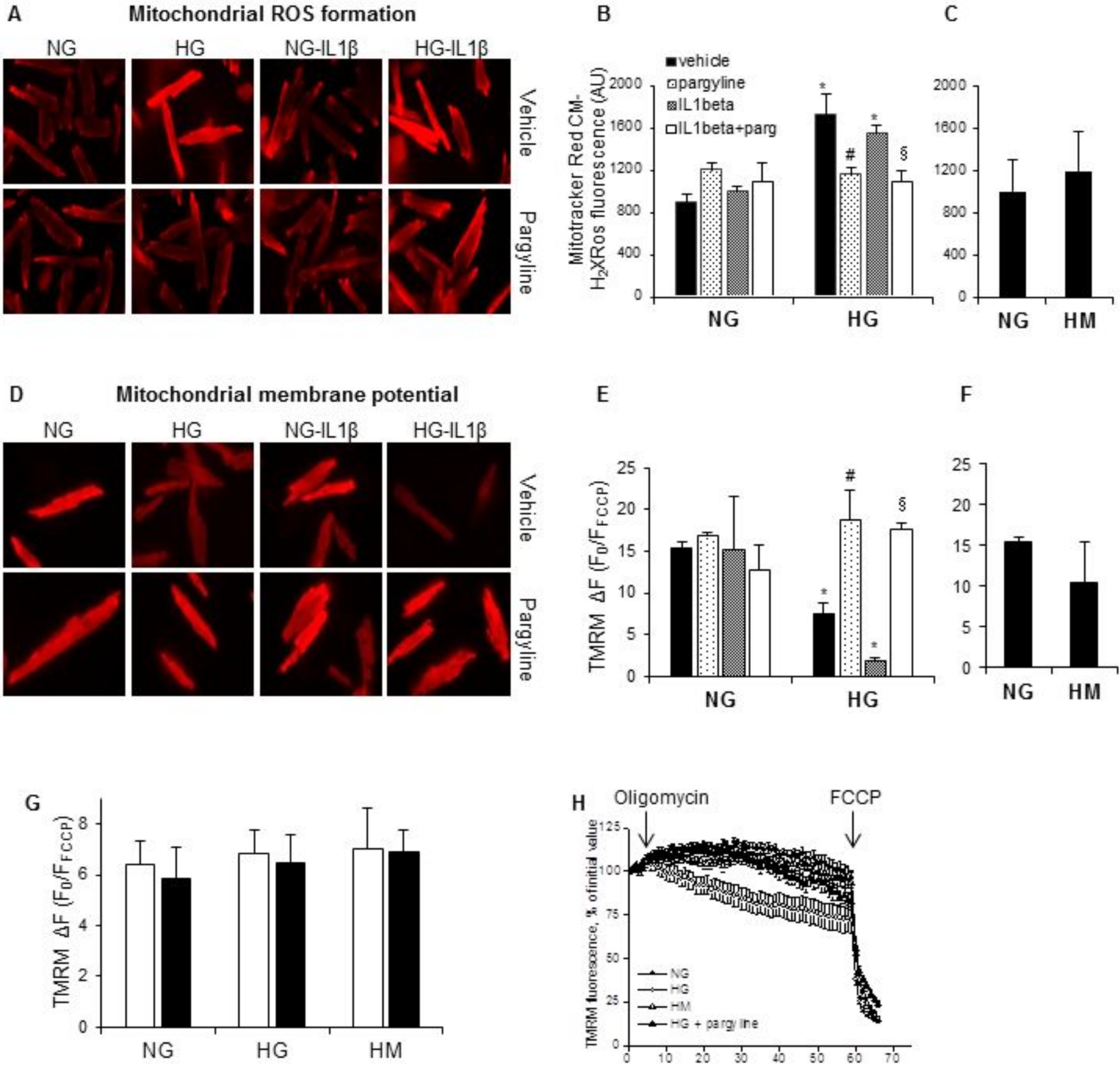
A
Mitochondrial ROS formation
NG
HG
NG-IL1β
HG-IL1β
Vehicle
Pargyline
B
vehicle
pargyline
IL1beta
IL1beta+parg
Mitotracker Red CM-H2XRos fluorescence (AU)
NG
HG
C
NG
HM
D
Mitochondrial membrane potential
E
TMRM ΔF (F0/FFCCP)
F
G
H
Oligomycin
FCCP
TMRM fluorescence, % of initial value
NG
HG
HM
HG + pargyline

**FIGURE 2**

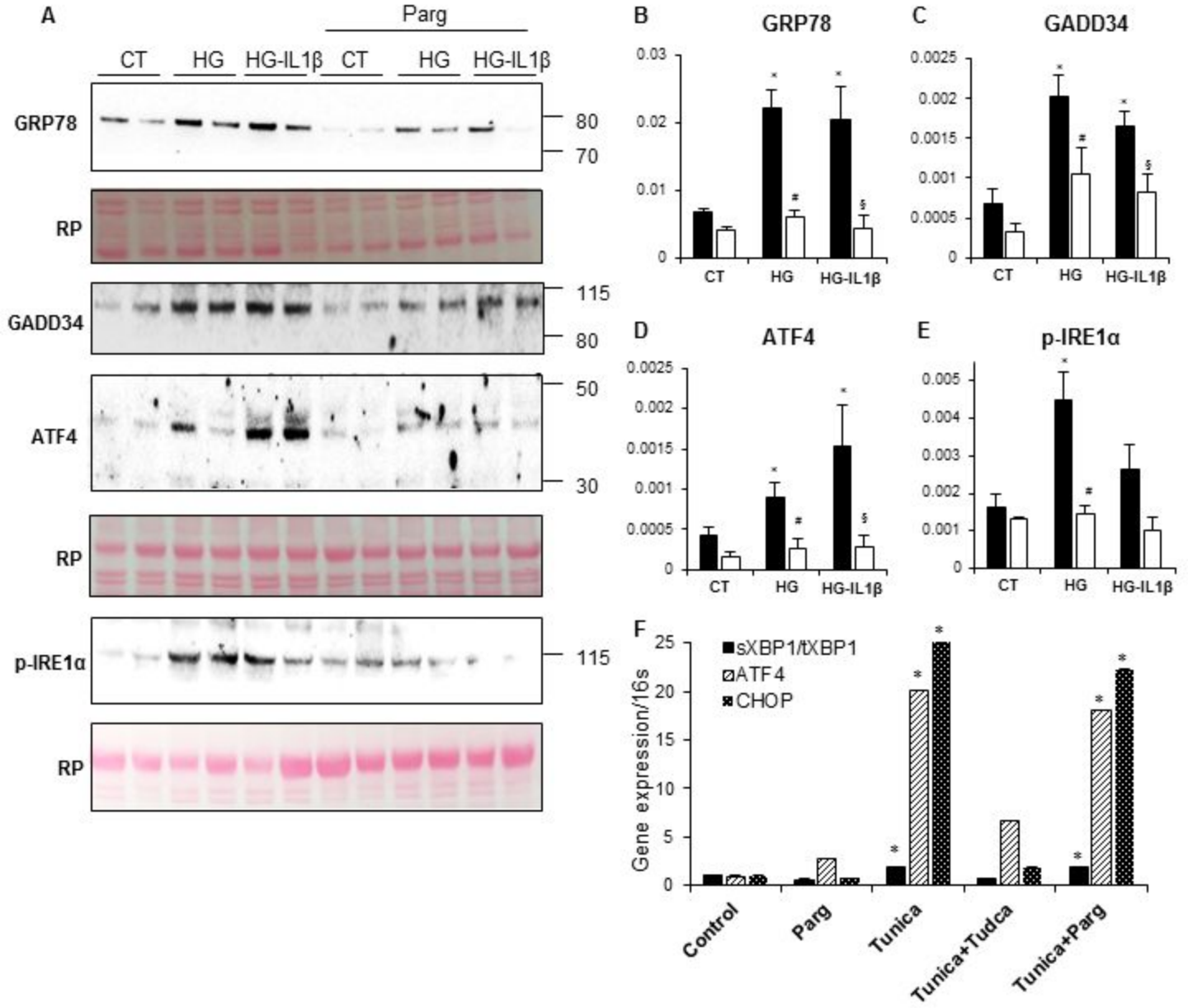
A
Parg
CT
HG
HG-IL1β
CT
HG
HG-IL1β
GRP78
80
70
RP
GADD34
115
80
ATF4
50
30
RP
p-IRE1α
115
RP
B
GRP78
C
GADD34
D
ATF4
E
p-IRE1α
F
sXBP1/tXBP1
ATF4
CHOP
Gene expression/16s
Control
Parg
Tunica
Tunica+Tudca
Tunica+Parg

**FIGURE 3**

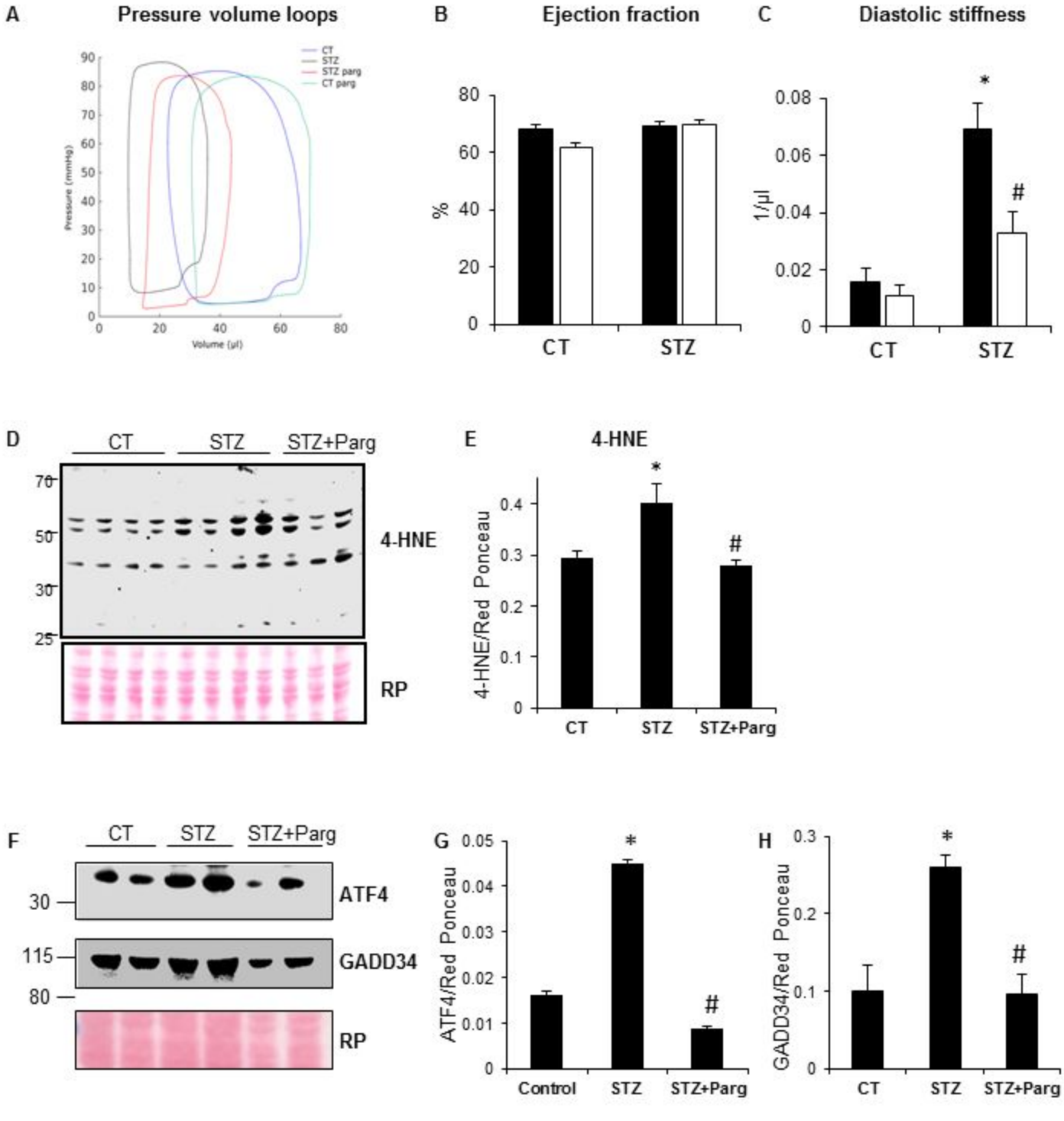
A
Pressure volume loops
CT
STZ
STZ parg
CT parg
Pressure (mmHg)
Volume (µl)
B
Ejection fraction
%
CT
STZ
C
Diastolic stiffness
1/µl
*
#
CT
STZ
D
CT
STZ
STZ+Parg
70
50
30
25
4-HNE
RP
E
4-HNE
4-HNE/Red Ponceau
*
#
CT
STZ
STZ+Parg
F
CT
STZ
STZ+Parg
30
115
80
ATF4
GADD34
RP
G
ATF4/Red Ponceau
*
#
Control
STZ
STZ+Parg
H
GADD34/Red Ponceau
*
#
CT
STZ
STZ+Parg

**FIGURE 4**

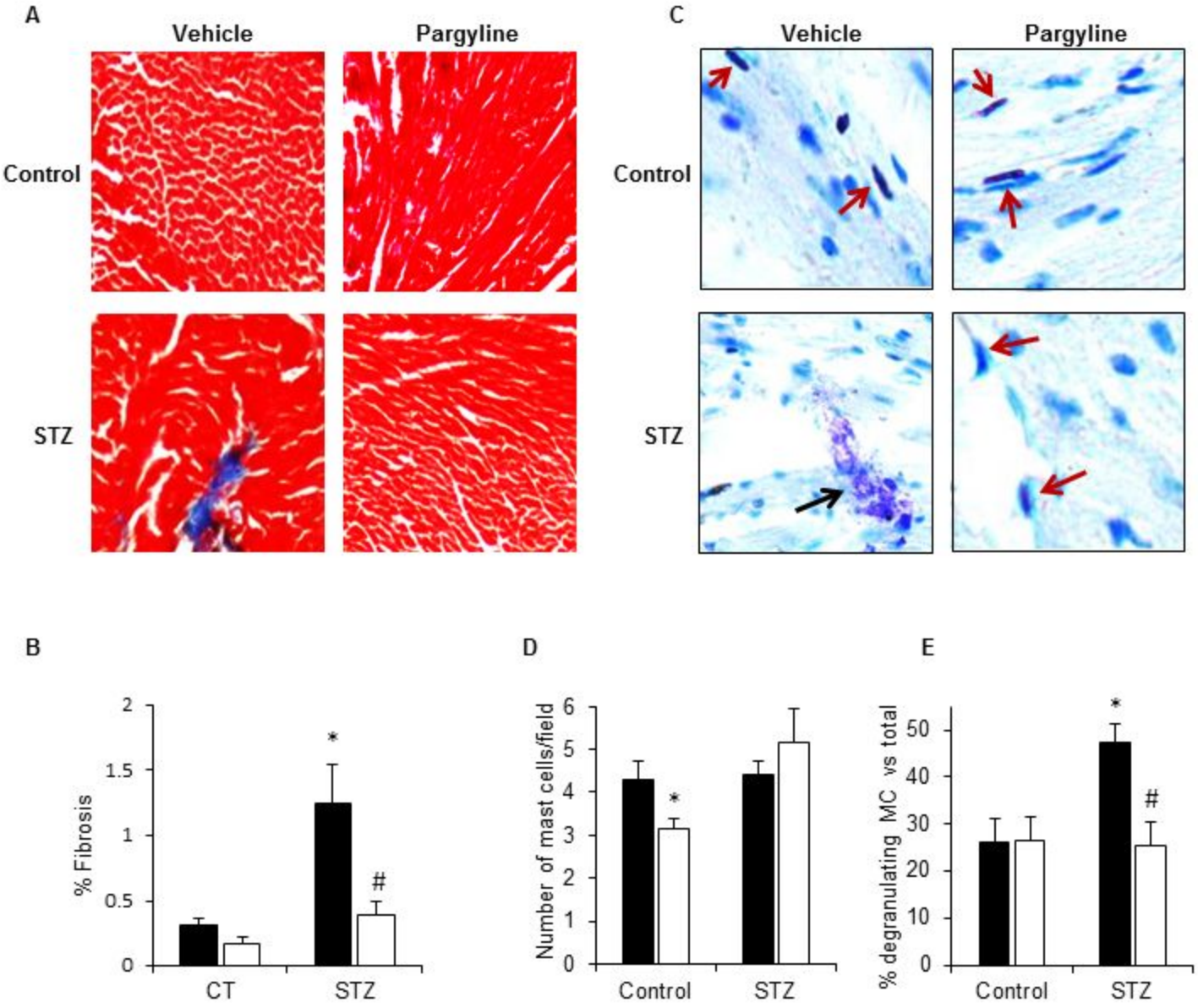
A
Vehicle
Pargyline
Control
STZ
C
Vehicle
Pargyline
Control
STZ
B
% Fibrosis
2
1.5
1
0.5
0
*
#
CT
STZ
D
Number of mast cells/field
6
5
4
3
2
1
0
*
Control
STZ
E
% degranulating MC vs total
50
40
30
20
10
0
*
#
Control
STZ

**FIGURE 5**

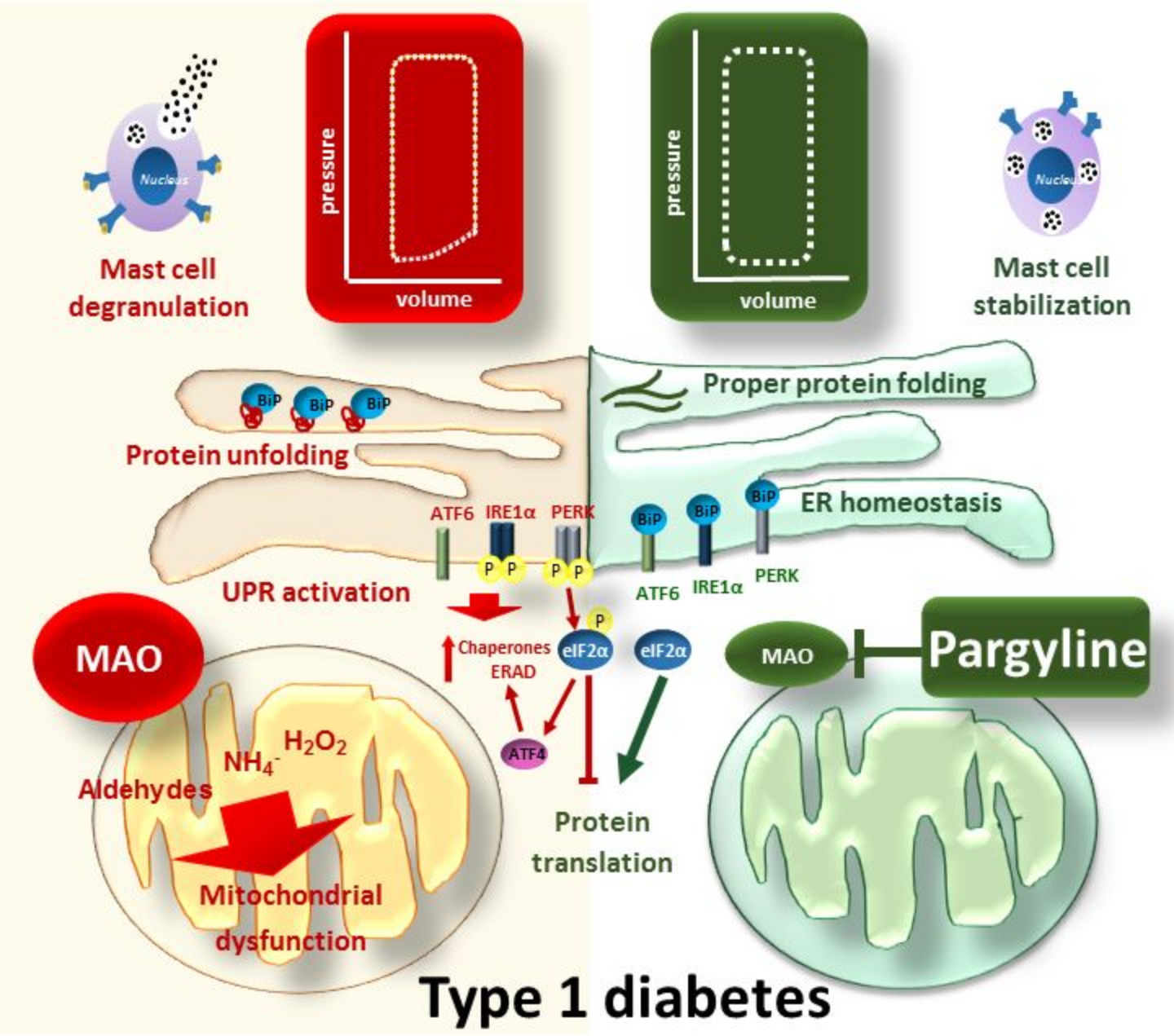
Mast cell degranulation
pressure
volume
pressure
volume
Mast cell stabilization
Nucleus
Nucleus
BiP
BiP
BiP
Protein unfolding
Proper protein folding
ATF6
IRE1α
PERK
ER homeostasis
BiP
BiP
BiP
ATF6
IRE1α
PERK
UPR activation
P
P
P
P
P
Chaperones
ERAD
eIF2α
eIF2α
MAO
Pargyline
MAO
ATF4
$NH_4^-$
$H_2O_2$
Aldehydes
Protein translation
Mitochondrial dysfunction
Type 1 diabetes

**FIGURE 6**